Supporting Material

Systematic heterogeneity of fractional vesicle pool sizes and release rates of hippocampal synapses

Oliver Welzel[*], Andreas W. Henkel[*,†], Armin M. Stroebel, Jasmin Jung, Carsten H. Tischbirek, Katrin Ebert, Johannes Kornhuber, Silvio O. Rizzoli[‡] and Teja W. Groemer[§]

Department of Psychiatry and Psychotherapy, University of Erlangen-Nuremberg, Schwabachanlage 6, 91054 Erlangen, Germany

[†] Department of Physiology, Faculty of Medicine, Jabriya, Kuwait University, P.O. Box 24923, Safat 13110, Kuwait

[‡] European Neuroscience Institute Göttingen (ENI-G), DFG Research Center for Molecular Physiology of the Brain (CMPB)/Excellence Cluster 171, Grisebachstrs. 5, 37077 Göttingen, Germany

[§] *Correspondence should be addressed to:*
Dr. Teja W. Groemer
Phone: +49 9131 85 44781
Fax: +49 9131 85 36381
E-mail: teja.groemer@uk-erlangen.de

[*] These authors contributed equally to this work

Supplemental Materials and Methods

Data analysis

All image and data analysis was performed using custom-written routines in MATLAB (The MathWorks, Natick, MA). The mean background determined from the intensity histogram of recorded image stacks was subtracted (1) and the resulting image stacks were used to automatically define peak regions of interest (ROI) of synaptic bouton size (2), where stimulation-evoked fluorescence decrease occurred in difference images. The average of each ROI was calculated for each image to obtain fluorescence intensity profiles. For the determination of the total pool size ΔF_{tot} the mean of five values after the total destain period was subtracted from the mean of five values before the onset of the stimulus. The readily releasable pool size was determined by subtraction the mean of five values after the 40 pulses stimulation period from the mean of five values before the onset of the stimulus. The half-decay time t_{50} for stimulation-induced fluorescence decrease was determined as follows: In a first step the minimum was subtracted. Second the parameters *a* and *b* of a single exponential function $a \cdot \exp(-b \cdot t)$ were estimated using a least squared error fit to each fluorescence profile. Fit results with a coefficient of determination below 0.8 were discarded. In a last step the half-decay time t_{50} was calculated by $t_{50} = \frac{\ln 2}{b}$ to determine the value where the fluorescence decayed to 50 % of its initial value during the first stimulation period with 600 pulses. For the generation of the half-decay time image, shown in Fig. 1 A, the above described calculation of t_{50} was executed for every pixel in the entire time-series. In the resulting half-decay time image the extreme values were cut and additionally the image was filtered with an average filter with a size of 3 pixels.

Statistical analysis was performed by MATLAB (The MathWorks, Natick, MA). Relations between total recycling pool size and readily releasable pool size were fitted with a linear model ($m_{linear} \cdot x$) or a power relationship ($m_{power} \cdot x^{2/3}$). m_{linear}, m_{power} and corresponding 95 % confidence intervals of the fitted functions are given, respectively (see Fig. 6 and Fig. S8). To test for differences in the groups of the binned illustration a one-way ANOVA was performed (see Fig. 1 C). Furthermore Spearman's rank correlation coefficient ρ between two parameters was calculated. To clarify the statistical results obtained ANOVA we used the effect size *d* (3) as a sample size independent measure, which specifies the quantity of an effect. We calculated Cohen's *d* always between the first and the last bin by: $d = \frac{\bar{x}_f - \bar{x}_e}{\sqrt{(s_f^2 + s_e^2)/2}}$,

where $\overline{x}_f$ and s_f are the mean and the standard deviation of the first bin and $\overline{x}_e$ and s_e are the estimated mean and standard deviation of the last bin, respectively. In benchmark tests for the determination of the half-decay time t_{50} we used the coefficient of variation, which is defined by: $\frac{s}{\overline{x}}$, where $\overline{x}$ is the mean and s the standard deviation. When a continuous distribution is described, it might be useful to introduce the terms "high values" and "low values" in order to emphasize differences in their individual properties. Accordingly, we discriminated between "synapses with large recycling pool sizes" and "synapses with small recycling pool sizes" that we defined as synapses with the highest or lowest 10 % of recycling vesicle numbers. Differences in the chosen recycling pool size groups (see Fig. 1 D) were tested using two-sample t-test. Levels of significance p (p-values) are indicated as follows: * $p < 0.05$, ** $p < 0.01$ and *** $p < 0.001$.

Computer simulations

Computer simulations on synaptic exocytosis were done, mainly to exclude signal-to-noise ratio (SNR), statistical and system-specific artifacts (see Fig. S5). In benchmark tests for the half-decay time determination and the peak detection method we simulated images I of size 100 x 100 pixels, each containing 10 randomly distributed spots of rotation symmetric Gaussian shape: $\exp\left(-\frac{1}{2}\frac{(x-\mu_x)^2+(y-\mu_y)^2}{\sigma^2}\right)$, where μ_x and μ_y are randomly chosen locations between 10 pixels and 90 pixels and σ is the standard deviation, randomly distributed between 1.38 and 2.58 pixels. Each image stack consisted of 100 images. For the influence of signal-to-noise ratio on the number of detected spots and on the determination of t_{50} we used the following parameters: a constant t_{50} of 10 s and an amplitude of each spot of 100. To achieve different SNR we varied the mean and the standard deviation of the added white Gaussian noise. The mean ranged from 1 to 51 with a step size of 2 and the standard deviation was always one third of the mean. SNR is calculated as follows: $\mathrm{SNR} = \left(\sum_{x,y=1}^{n} I^2(x,y)\right)^{0.5}\left(\sum_{x,y=1}^{n} I_n^{\,2}(x,y)\right)^{-0.5}$ (4), where x, y are the coordinates of the image, n is the size of the square image and I_n is the added Gaussian white noise image. Using the above definition of SNR we achieved SNR values ranging from 1.05 to 9.78. All SNR values were calculated for the first image of the simulated stacks as they dropped with

further images because of the single exponential decay of each spot. We simulated 20 image stacks and thus obtained 200 independent measurements for each SNR.

The benchmark test for the estimation of different half-decay times t_{50} was carried out with images of size 100 x 100 containing 10 spots of rotation symmetric Gaussian shape with standard deviations between 1.38 and 2.58, which was randomly distributed between 10 pixels and 90 pixels. Each image stack consisted of 350 images. The initial amplitude of each spot was 100 and the mean of additive Gaussian white noise was 10 with a standard deviation of 5 resulting in average SNR of 1.44 for all 20 image stacks. The default for half-decay times ranged from 4 s to 100 s with a step size of 4 s.

For direct comparison between real data and simulation we generated image stacks of 50 images of size of 100 x 100 pixels containing 10 randomly distributed spots of rotation symmetric Gaussian shape with standard deviations between 1.38 and 2.58 pixels. To each image Gaussian white noise with mean 250 and standard deviation 25 was added, which is in good agreement with the real background data obtained from the FM dyes experiments. Each spot exhibited a single exponential decay time of 6.6 s, which approximately corresponds to the mean of the measured data from FM 1-43 experiments stimulated at 30 Hz (see Fig. 1 B). The initial amplitude of each spot varied randomly between 500 and 14500 and thus in the range of camera dynamics. We simulated 500 of those image stacks resulting in 5000 simulated boutons. These stacks were used for peak detection and the subsequent determination of fluorescence kinetics parameters, especially this for the half-decay time t_{50}. Note that peaks were randomly distributed as in real data and thus not all simulated spots were detected as e.g. some spots localized close to each other. We detected 4376 of the 5000 simulated spots.

Supplemental Figures

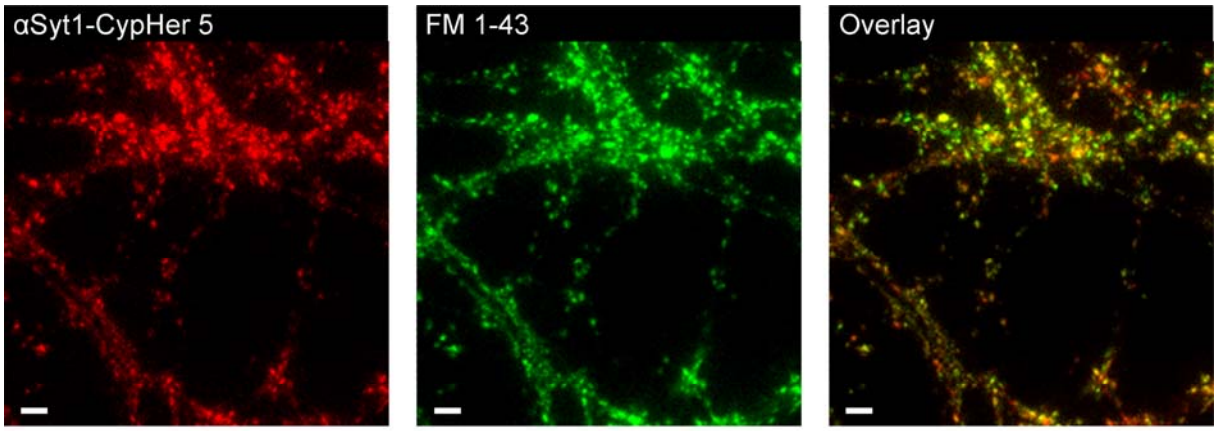

Pearson's correlation	Mander's overlap	Mander's overlap coefficients k_1, k_2	Colocalization coefficients c_1, c_2
0.86 ± 0.0007	0.94 ± 0.007	k_1 = 0.94 ± 0.01 k_2 = 0.94 ± 0.03	c_1 = 0.9995 ± 0.0001 c_2 = 0.9995 ± 0.0001

FIGURE S1. Colocalization of αSyt1-CypHer 5 and FM 1-43. Representative fluorescence images of αSyt1-CypHer 5 (red), FM 1-43 (green) and corresponding overlay. Corresponding colocalization coefficients are given in table below (3 experiments; scale bars 4 μm).

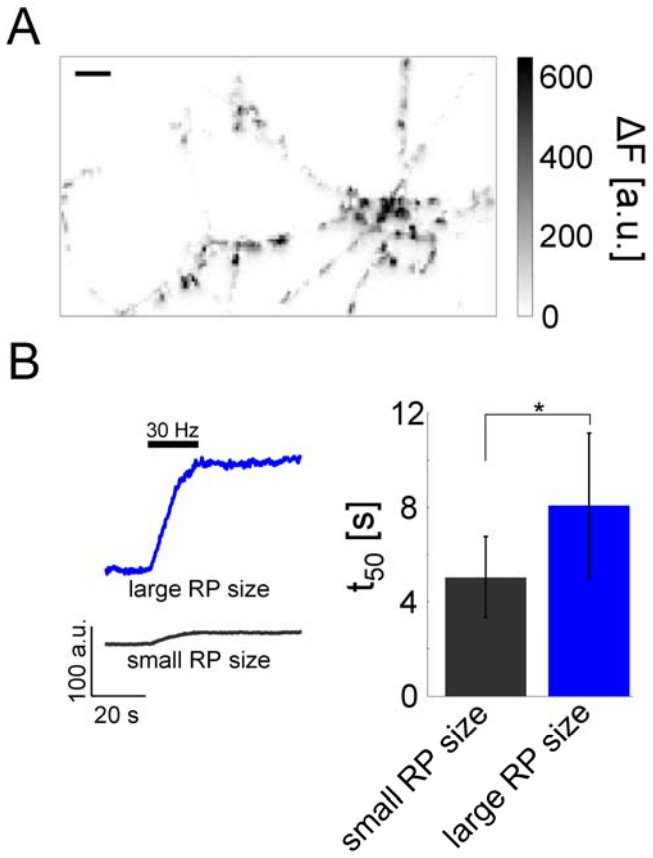

FIGURE S2. Relation between recycling pool (RP) size and electrically evoked synaptopHluorin fluorescence increase time constant t_{50}. (A) Difference-image of neurons transfected with synaptopHluorin in a typical experiment (Scale bar 6 µm). (B) Presynaptic terminals were stimulated with 600 pulses at 30 Hz in the presence of folimycin to block re-acidification. The time constant t_{50} increases with increasing fluorescence change ΔF (Spearman's $\rho = 0.43 \pm 0.10$, $p < 0.05$; Cohen's $d = 0.81 \pm 0.37$) Synapses with large RP sizes released their dye content relatively slower than synapses with small RP sizes (two-sample t-test: * $p < 0.05$; 92 synapses, 3 experiments). Error bars indicate standard error of the mean.

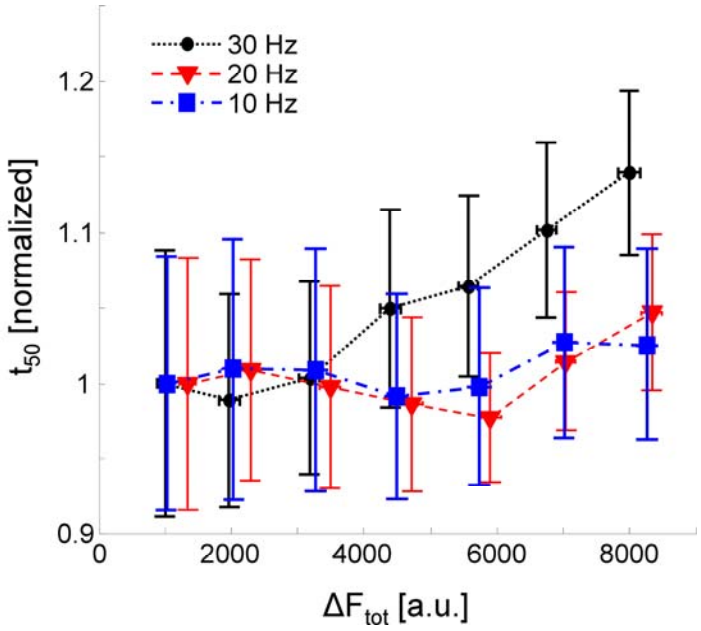

FIGURE S3. The correlation between recycling pool size ΔF_{tot} and half-decay time t_{50} for different stimulation frequencies (10 Hz, 20Hz and 30 Hz). The positive correlation for 30 Hz stimulation (black circles; Spearman's $\rho = 0.23 \pm 0.07$, $p < 0.05$) vanished when reducing stimulation frequency to 20 Hz (red triangles; Spearman's $\rho = 0.09 \pm 0.03$, $p > 0.15$; 3092 synapses, 5 experiments) and 10 Hz (blue squares; Spearman's $\rho = 0.01 \pm 0.04$, $p > 0.3$; 2010 synapses, 3 experiments), respectively. Error bars indicate standard error of the mean of ΔF_{tot} and t_{50} for each bin, respectively.

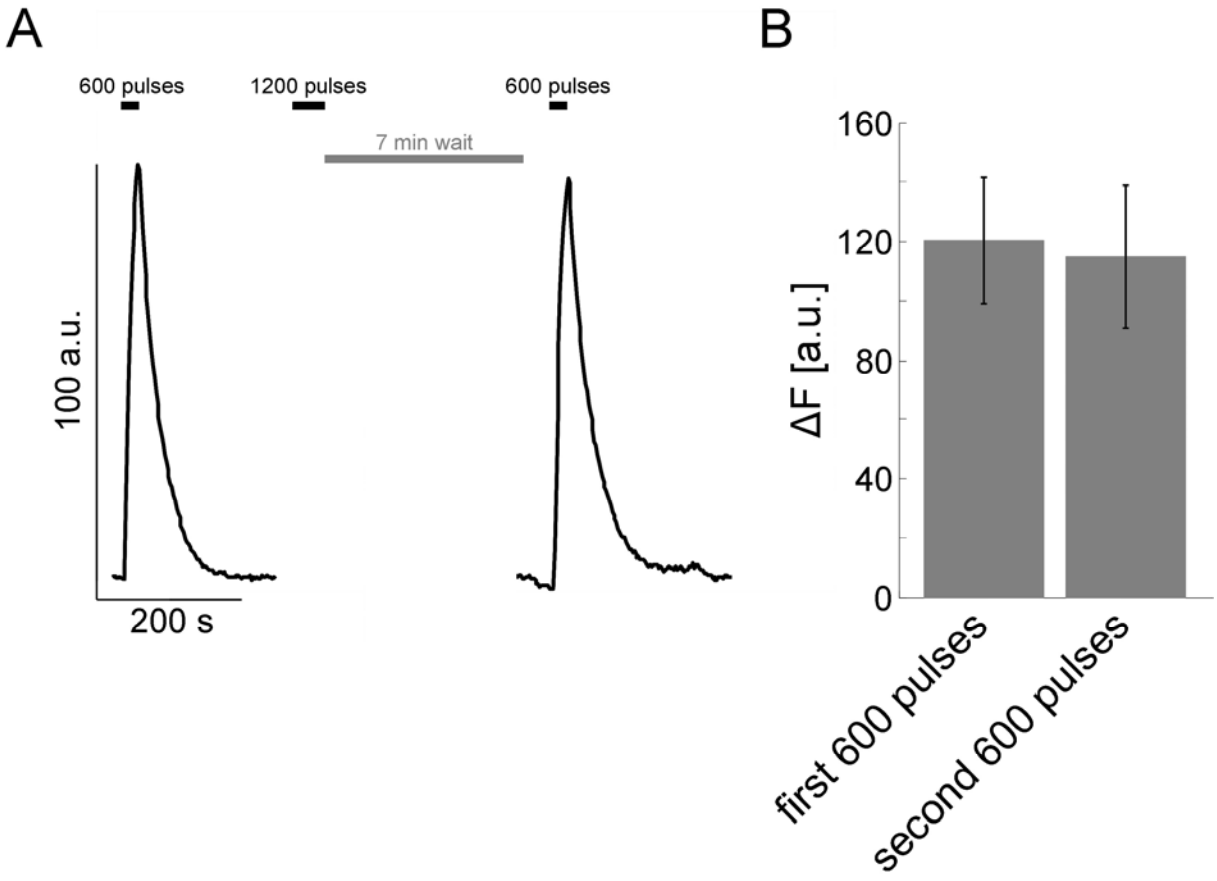

FIGURE S4. Loading stimulus used in FM dye experiments has no significant influence on the kinetics and pool sizes during experiment time. (A) Mean fluorescence profiles of preparations transfected with synaptopHluorin (1265 synapses, 6 experiments). Presynaptic terminals were first stimulated with 600 pulses at 30 Hz, which was used as the reference stimulus. Afterwards cells were stimulated with 1200 pulses at 40 Hz, which correspond to maximal loading in FM dye experiments. After waiting for 7 min, which was the time used for washing in FM dye experiments, 600 pulses at 30 Hz were delivered again. (B) Comparison of fluorescence changes ΔF of the reference stimulus and the second 600 pulses stimulus (two-sample t-test: $p = 0.85$). Furthermore exocytosis and endocytosis kinetics were not statistically different (exocytosis: 10.46 s ± 2.25 s and 10.14 s ± 1.06 s; two-sample t-test: $p = 0.76$; endocytosis: 20.44 s ± 6.42 s and 22.35 s ± 4.14 s; two-sample t-test: $p = 0.55$). Error bars indicate standard error of the mean.

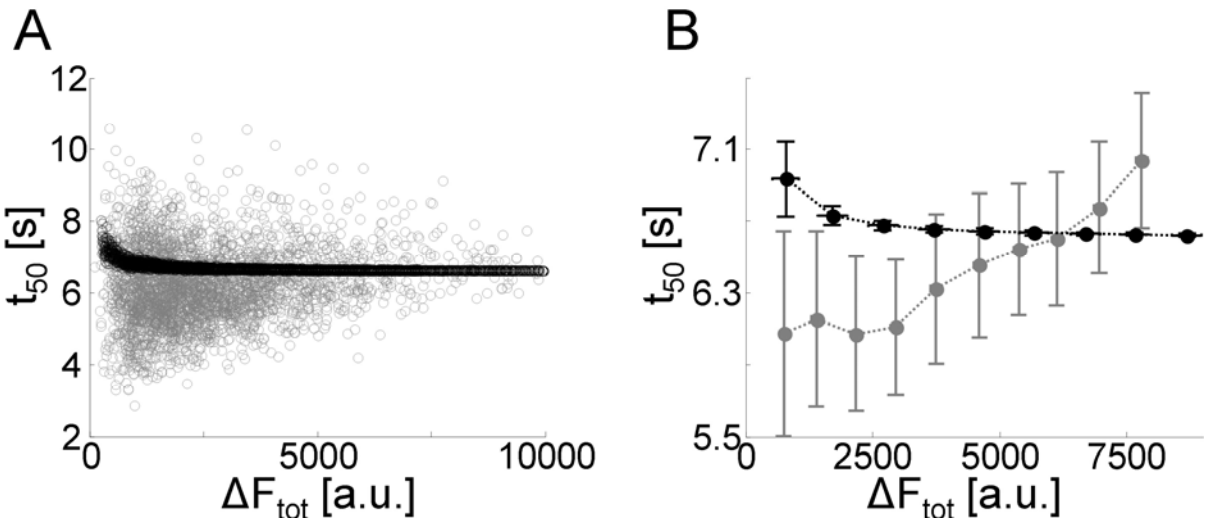

FIGURE S5. Computer model simulations of half-decay time t_{50} determination. The correlation between recycling pool size ΔF_{tot} and half-decay time t_{50} are not compromised by statistical and analysis-specific appraisal artefacts. (A) In simulations a first order exponential function with a fixed half-decay time of 6.6 s was used for each simulated spot. Recycling pool size ΔF_{tot} versus half-decay time t_{50} for each measured synapse (gray circles; 3149 synapses, 5 experiments) and for simulated data (black circles, n = 4376), respectively. (B) Experimental and simulation data from (A) were grouped in bins and averaged. Error bars indicate standard error of the mean of ΔF_{tot} and t_{50} for each bin, respectively.

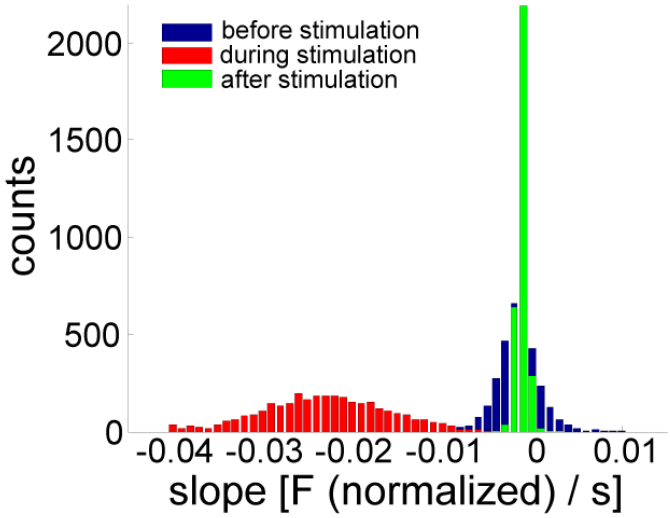

FIGURE S6. Histogram of slopes corresponding to linear fits to normalized fluorescence profiles from 3176 synapses. Slopes during stimulation (red) can be well separated from those before (blue) and after stimulation (green), respectively. Additionally bleaching is limited to less than 7 % of the fluorescence decrease, which is still an overestimate as the slope decreased with time.

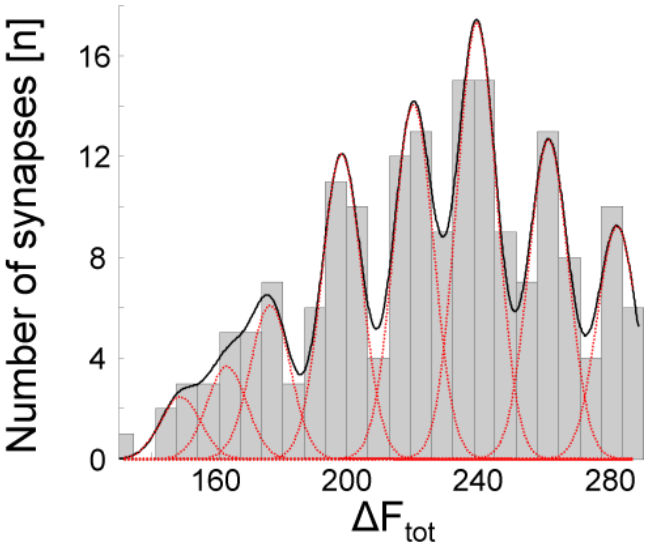

FIGURE S7. Determination of single synaptic vesicle fluorescence. Histogram of ΔF_{tot} values of 181 boutons loaded with 20 pulses. Solid black line is a multiple Gaussian fit with peaks at almost equal 20 a.u. intervals. Single Gaussians with equal widths are represented by red dotted lines. To determine the number loaded quanta, the mean interval between the centres of the Gaussian peaks were used. Using this approach we determined the mean fluorescence of a single vesicle to 20.02 ± 1.91 a.u. (613 synapses, 3 experiments).

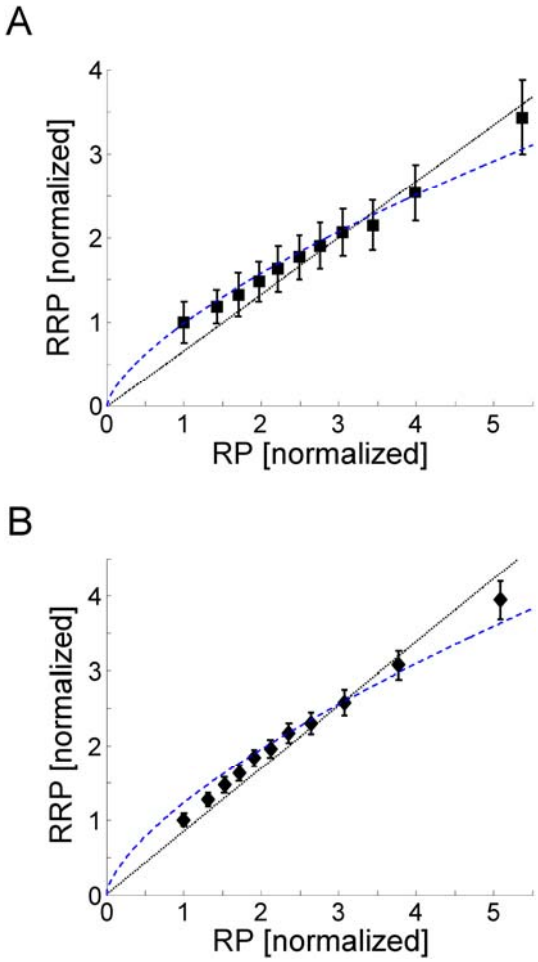

FIGURE S8. The relation between readily releasable pool (RRP) and recycling pool (RP) size obtained from synaptopHluorin and αSyt1-CypHer 5 experiments fits to a volume to surface dependency, described by a power function: $m_{power} \cdot x^{2/3}$. (A) SynaptopHluorin: A linear fit (dashed black line, m_{linear} = 0.67 (0.63, 0.71)) and a power function (dashed blue line, m_{power} = 1.00 (0.96, 1.05)) are shown. (B) αSyt1-CypHer 5: A linear fit (dashed black line, m_{linear} = 0.84 (0.80, 0.89)) and a power function (dashed blue line, m_{power} = 1.23 (1.17, 1.28)) are shown. In synaptopHluorin and αSyt1-CypHer 5 experiments the RRP increases nonlinearly with the RP. Error bars indicate standard error of the mean.

Supplemental Table

Fitmodel	$y = m_{power} \cdot x^{2/3}$	$y = m_{linear} \cdot x$
R^2	0.9874	0.8020
95% confidence bounds for m	0.9272, 0.9808	0.5836, 0.7318
Lilliefors test	$p > 0.5$	$p = 0.32$
Wald-Wolfowitz runs Test	$p = 0.4585$	$p = 0.0183$
Schwarz-Bayes criterion	29.86	30.20

TABLE T1. Statistics for the power function fit and the linear fit of Fig. 6.

References

1. Stroebel, A., O. Welzel, J. Kornhuber, and T. W. Groemer. 2010. Background determination-based detection of scattered peaks. Microscopy Research and Technique.
2. Sbalzarini, I. F., and P. Koumoutsakos. 2005. Feature point tracking and trajectory analysis for video imaging in cell biology. J Struct Biol 151:182-195.
3. Cohen, J. 1988. Statistical Power Analysis for the Behavioral Sciences. Lawrence Erlbaum Assoc Inc.
4. Welzel, O., D. Boening, A. Stroebel, U. Reulbach, J. Klingauf, J. Kornhuber, and T. W. Groemer. 2009. Determination of axonal transport velocities via image cross- and autocorrelation. Eur Biophys J 38:883-889.